International Seminar of Research Month
Science and Technology for People Empowerment
Volume 2018

NST PROCEEDINGS
OPEN ACCESS

Conference Paper

Study of Comparison of Salinity Value in Coastal of Sampang District Using Aqua Modis Satellite Image Data

S. Zainab*, D. P. Solin

Civil Engineering, Faculty of Engineering, Universitas Pembangunan Nasional "Veteran" Surabaya, East Java, Indonesia

Abstract

Salinity is one of the parameters that used for detecting the changes in ecosystems in shallow sea water. The high and low salinity will affect the lives of vegetation and animals. Identifying the salinity content of Sampang District is highly needed considering that Sampang District is well-known producer and exporter of salt. This study was emphasized in mapping the salinity value by using remote sensing algorithms. The mathematic models that used in this research are linear, exponential, logarithm, and power models. The result of this research shows that mapping by using level-2 aqua satellite image is well applied. The result shows that using wavelength 443 mm and 531 mm of Aqua Modis data presents the highest correlation values. The optimum regression for these two wavelength are Sal(ppt)=8,15*ln(Rrs_443)+66,128 with the value R^2 as 0,8736 and Sal(ppt)= 8,15 *ln(Rrs_443) + 64,611 with the correlation value R^2 as 0,8322. From these result, it can be concluded that there are no significant differences satellite image data for salinity to the data acquisition time.

Keywords: Aqua Modis, mathematical models, remote sensing, salinity

INTRODUCTION

A healthy aquatic environment plays an important role and vital to marine life. For observing the healthy aquatic environment, there are several ways that have been obtained. Salinity checking is one of the accurate ways to identify the aquatic environment. In brief, a high salinity value will cause interference in the aquatic environment which means most of the sea creature could not survive and grow well in high salinity. Vice versa with low salinity value, it can be said that there would be a lack of nutrients elements in the aquatic environment. This condition is not good enough for the living of sea creatures because as is well known, the salt content in a body of water is needed by all the sea creatures. (Anguelova & Huq, 2017; Asfaw, Suryabhagavan, & Argaw, 2016; Li, Hu, & Xia, 2013).

In salinity checking there are various ways to measure the salinity value in the body of water, those are total dissolved salt (TDS) and electrical conductivity (EC). Among these two methods, electrical conductivity is used more often. EC is also called as salinometer. Salinometer is compatible tools for measuring the salinity directly by dropping the water sample in the tools and result can be known directly from digital reading. However, for wide area coverage, this measurement requires a lot of time. Since it is quite difficult for checking the salinity at the same time and the limitation of time, using technology for monitoring the ecosystem changes is highly needed. This technology is remote sensing.

Remote sensing is one of technology for detecting and monitoring the surface of the area without making physical contact with the area. The remote sensing has the capability in monitoring a wide area in one measurement.

* Corresponding author
Email address: iinzainab@yahoo.com

How to cite this article: Zainab, S. & Solin, D. P (2018) Sutdy of Comparison of Salinity Value in Coastal of Sampang District Using Aqua Modis Satellie Image Data. *International Seminar of Research Month Science and Technology for People Empowerment*. NST Proceedings. pages 333-342.doi: 10.11594/nstp.2019.0245.

The results of this measurement are shown in digital numeric values. It can be converted into reflectance values which are useful for predicting changes in each of the parameters that occur in the area studied (Petitcolin & Vermote, 2001; Zhou et al., 2018).

Nowadays, there are several studies that discuss the salinity value of seawater using remote sensing technology. Sensor technology developed in remote sensing has different levels of resolution starting with AVHRR sensors (Mittaz & Harris, 2011; Wang & Cao, 2008), satellite GOES (Jiménez-Muñoz & Sobrino, 2008), Terra and Aqua Modis (Mathew , Srinivasa Rao, & Mandla, 2017; Moreno-Madrinan, Al-Hamdan, Rickman, & Muller-Karger, 2010; Ruello et al., 2017; Wibisana & Zainab, 2017) Meris, Landsat ETM + (Kumar, Bhaskar, & Padmakumari , 2012) and OLI Landsat (Guo et al., 2016; Lymburner et al., 2016).

Groundwater salinity is mostly used to detect salt water levels used to monitor cropping systems for farmers while seawater salinity is used as input to monitor seawater intrusion to the land which can affect pond water quality (Arabi, Salama, Wernand, & Verhoef, 2018; Lee, Fredolin, Isabella, & Saim, 2017).

In this study, the salinity value of Sampang district would be mapped for two different times (June and July). These two different times were used for identifying whether there was a significant change in the time and also for determining the distribution pattern of salinity horizontally along the coastal coast of the district Sampang.

METHODS

Taking the Materials

This research was carried out in coastal of Sampang district. This area was located in Madura island. At the beginning of this research, the location was pinned on maps. There is 20 coordinate that has been chosen to test. All 20 samples were carried out and tested in the laboratory.

Downloading Aqua Modis Satellite Image

Aqua fashionable satellite imagery is obtained from Nasa's webpage with the address https://oceancolor.gsfc.nasa.gov/. The Level 2 fashionable aqua satellite image was selected since these data already had a radiometric correction. Satellite image file names taken for the purposes of this study are image files in July 2018 with file names A2018215061500.L2_LAC_OC.nc and June 2018 with file names A2018185060000.L2_LAC_OC.nc. The appearance of fashionable aqua satellite imagery is made respectively for 443 nm, 531 nm, and 667 nm wavelengths that represent the visible wavelengths of light for RGB (red, green, blue). For July 2018, it is shown in Figure 1 and the display in June 2018 is shown in Figure 2.

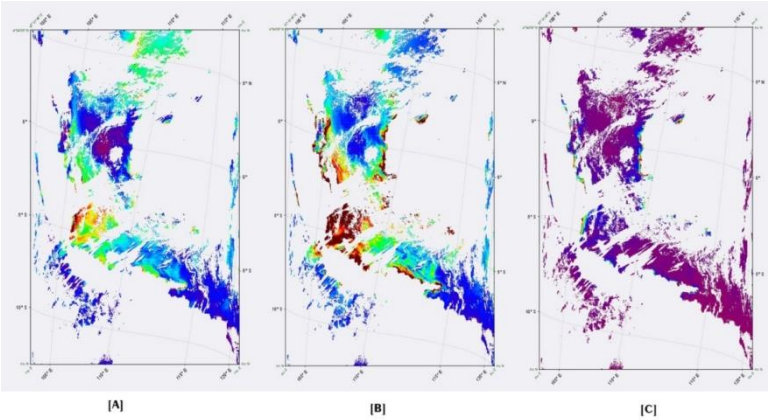

Figure 1. Aqua Modis satellite imagery in July 2018 at wavelengths 443,531 and 667 nm

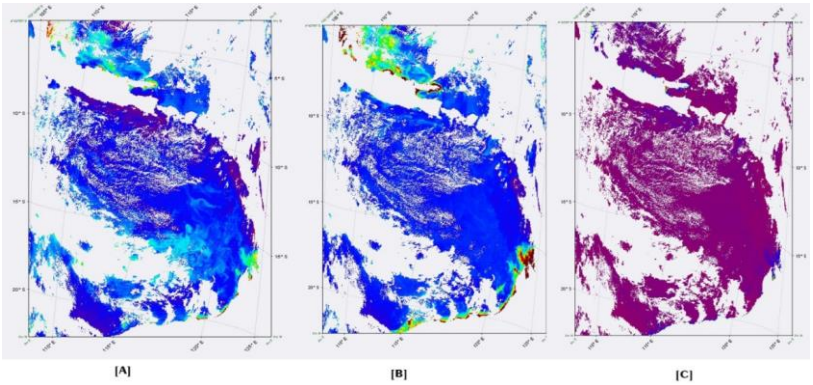

Figure 2. Aqua Modis satellite images in June 2018 at wavelengths 443,531 and 667 nm

Satelllite Image Cutting Process

The original image from the website presents the whole area of Madura Island. For obtaining the research location cropping is needed. The figure was cropped at the coordinates of -6.814o to -7.32o South Latitude and 112.505o to 114.3392o Longitude East and the results are shown in Figure 3., for July 2018 and Figure 4., for June 2018.

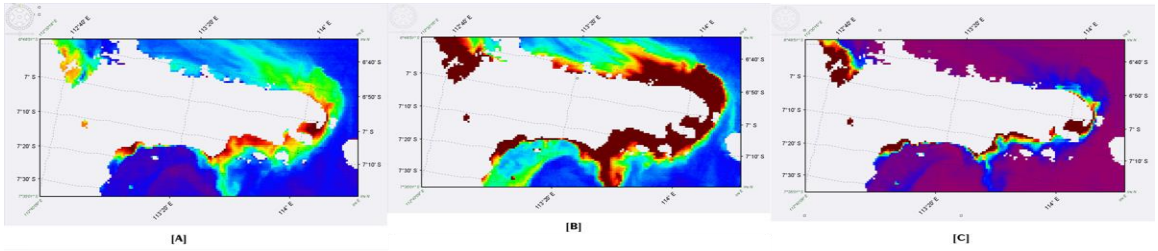

Figure 3. Aqua Modis Satellite Image from the Cutting Process of Downloaded Images for July 2018 for the Island Area of Madura and its Surroundings

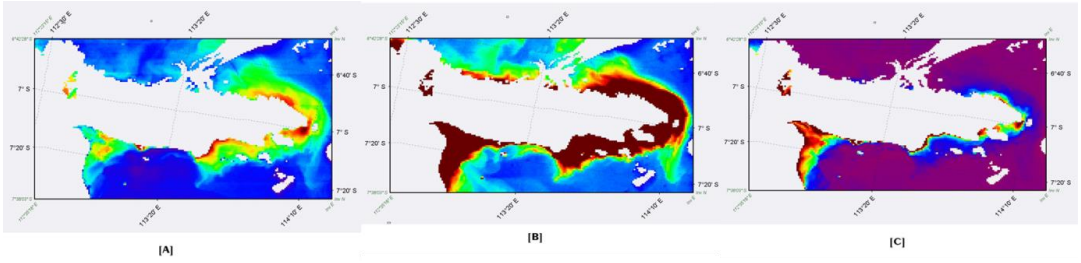

Figure 4. Aqua Modis Satellite Image from the Cutting Process of Downloaded Images for June 2018 on the Island Area of Madura and its Surroundings

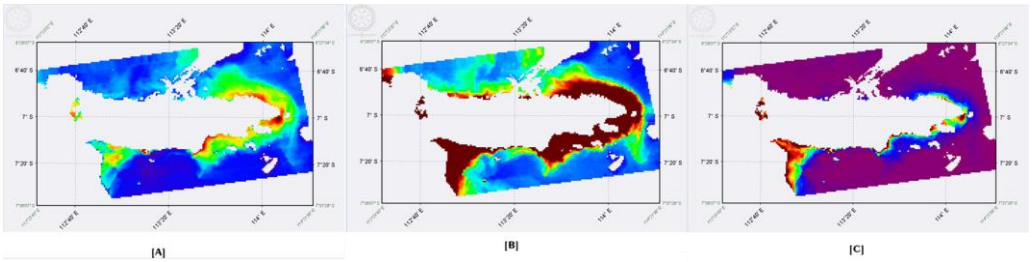

Figure 5. Aqua Modis satellite image after going through reprojection with WGS 84 and UTM 49S zone in July 2018

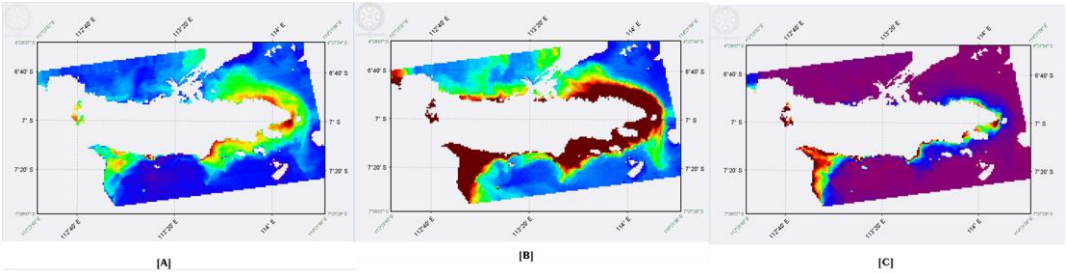

Figure 6. Aqua Modis satellite image after going through reprojection with WGS 84 and UTM 49S zone in June 2018

Determining Coordinate of Sample Points

The placement of the coordinates of the sample points is adjusted to the measurement of GPS navigation in the field when taking the salinity data on the coast, the results of the measurement of sample points are shown in Figure 7.

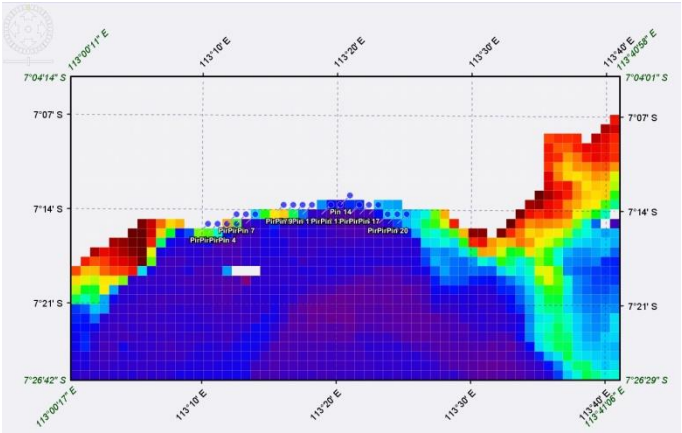

Figure 7. Setting the coordinates of sample points on the Aqua Modis satellite image for the coastal area of Sampang Madura district

RESULT AND DISCUSSION

From the measurement of salinity parameters using excel, the results of mathematical models are obtained with a correlation value R2 that shows the level of the relationship between the data and the mathematical model that exists. For measurements at a wavelength of 443 nm shown in Figure 8 and Table 1 which contains a resume of the existing mathematical models.

Table 1. The algorithm of mathematical models of Salinity at a wavelength of 443 nm

No	Algoritma	Model Mathematics	R^2
1	Linier	$y = 1576{,}1x + 13{,}198$	0,8205
2	Eksponensial	$y = 13{,}893e^{75{,}048x}$	0,7177
3	Logaritmik	$y = 8{,}1497\ln(x) + 66{,}128$	0,8736
4	Power	$y = 183{,}15x^{0{,}3986}$	0,8060

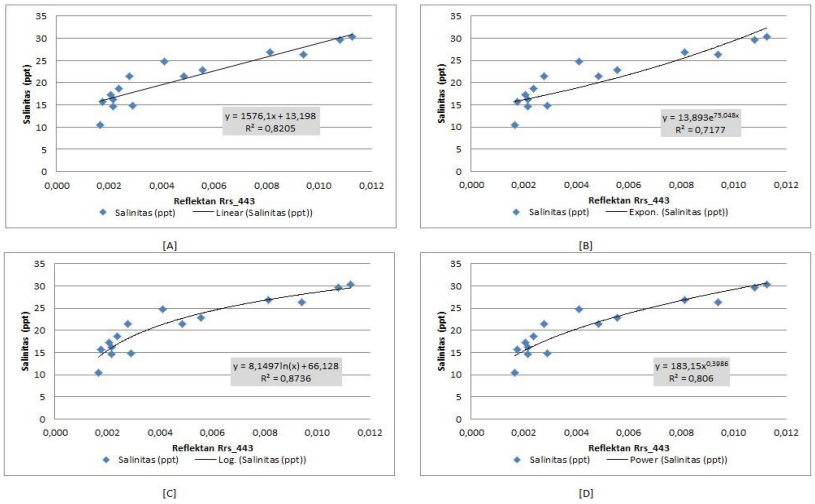

Figure 8. Results of scattering analysis Salinity of fashionable aqua images for wavelengths of 443 nm

Table 2. The algorithm of mathematical model Salinity at wavelength 531 nm

No	Algoritma	Model Mathematics	R^2
1	Linier	$y = 831{,}04x + 13{,}077$	0,7745
2	Eksponensial	$y = 13{,}818e^{39{,}534x}$	0,6761
3	Logaritmik	$y = 8{,}0501\ln(x) + 60{,}157$	0,7944
4	Power	$y = 135{,}56x^{0{,}3919}$	0,7262

Table 3. Mathematical Salinity model algorithm at a wavelength of 667 nm

No	Algoritma	Model Mathematics	R^2
1	Linier	$y = 767{,}68x + 17{,}056$	0,3463
2	Eksponensial	$y = 16{,}814e^{35{,}077x}$	0,2789
3	Logaritmik	$y = 2{,}4429\ln(x) + 35{,}118$	0,2247
4	Power	$y = 37{,}457x^{0{,}1075}$	0,1678

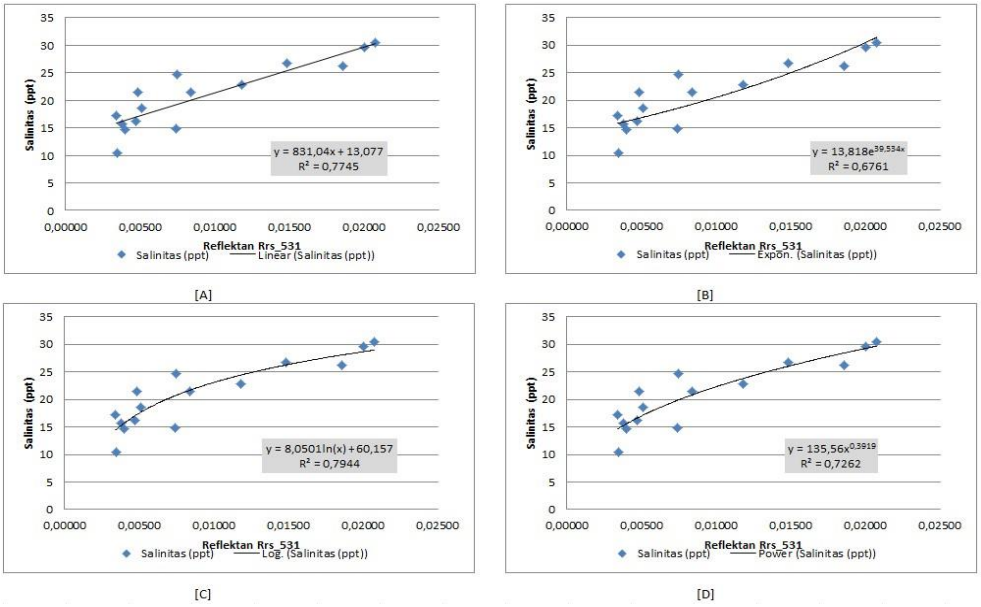

Figure 9. Results of scattering analysis Salinity of fashionable aqua images for a wavelength of 531 nm

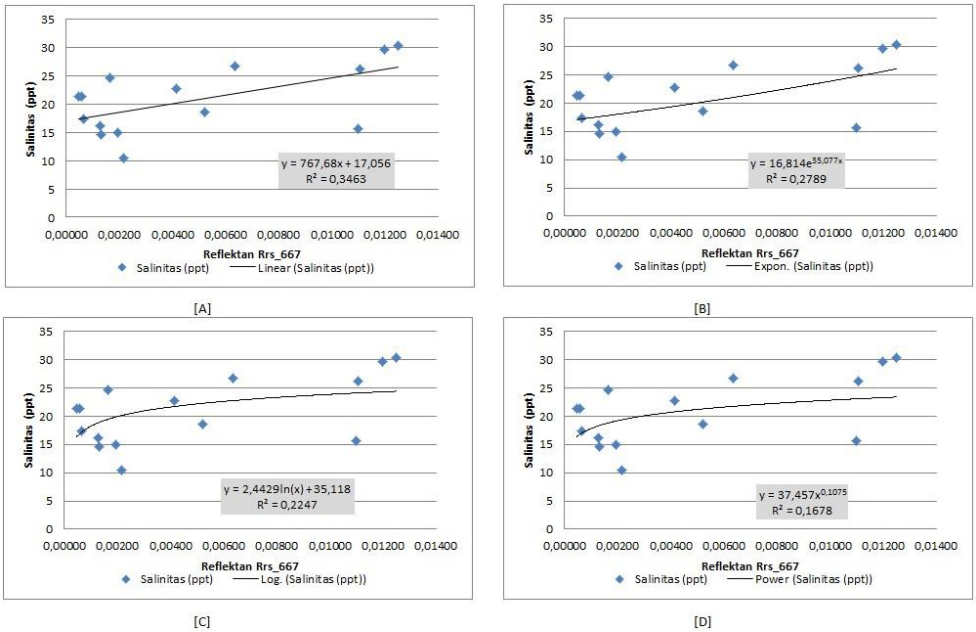

Figure 10. Results of scatter Salinity analysis of fashionable aqua images for a wavelength of 667 nm

Table 4. Fashionable aqua image reflectance data and Salinity value (ppt)

Longitude	Latitude	Rrs_443	Rrs_531	Rrs_667	Salinitas (ppt)
113,16227	-7,26290	0,01457	0,02574	0,01348	30,4
113,27937	-7,23892	NaN	NaN	NaN	26,3
113,29108	-7,23886	0,00325	0,00878	0,00194	22,8
113,31452	-7,23874	0,00277	0,00756	0,00930	18,6
113,32624	-7,23868	0,00249	0,00710	0,00658	15,7
113,33791	-7,22692	NaN	NaN	NaN	14,9
113,34969	-7,23856	0,00241	0,00463	0,00720	10,4
113,36140	-7,23850	0,00226	0,00499	0,00440	16,2
113,37312	-7,23844	0,00236	0,00512	0,00680	14,7
113,38490	-7,25008	0,00486	0,00656	0,00406	17,3
113,39662	-7,25001	0,00463	0,00626	0,00350	21,4
113,17399	-7,26284	0,01435	0,02544	0,01412	29,7
113,40834	-7,24995	0,00481	0,00658	0,00458	21,4
113,18572	-7,26278	0,01014	0,02012	0,00776	26,8
113,19743	-7,26273	0,00630	0,01389	0,00270	24,7
113,19738	-7,25102	0,01232	0,02397	0,01051	32,7
113,20910	-7,25096	0,00449	0,01015	0,00148	26,4
113,22082	-7,25091	0,00222	0,00526	0,00252	21,9
113,25592	-7,23904	0,01122	0,02429	0,01460	30,1
113,26765	-7,23898	NaN	NaN	NaN	31,5

Description: NaN: data not detected

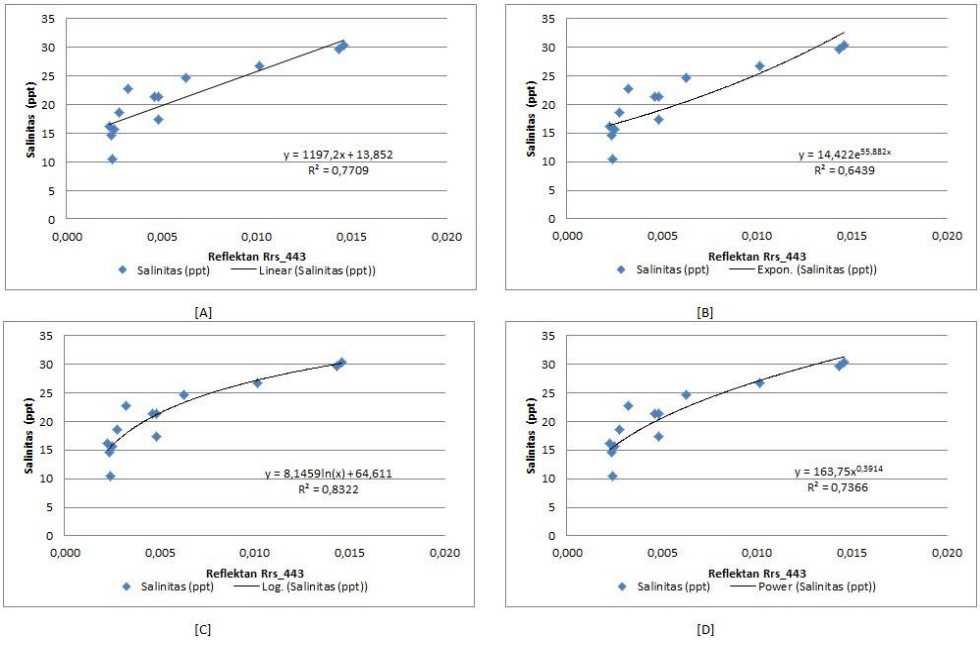

Figure 11. Results of scatter Salinity analysis of fashionable aqua images for wavelengths of 443 nm in June 2018

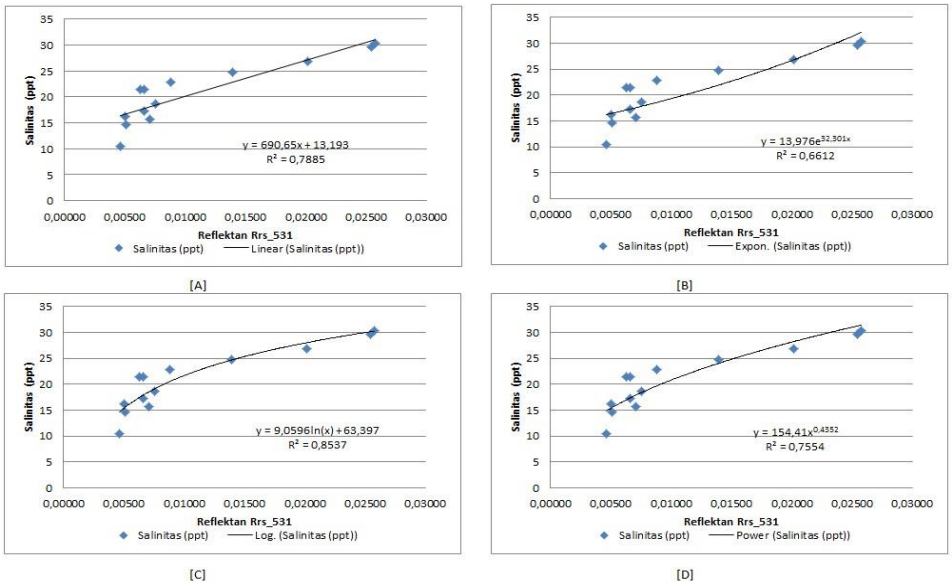

Figure 12. Results of scatter Salinity analysis of fashionable aqua images for wavelengths of 531 nm in June 2018

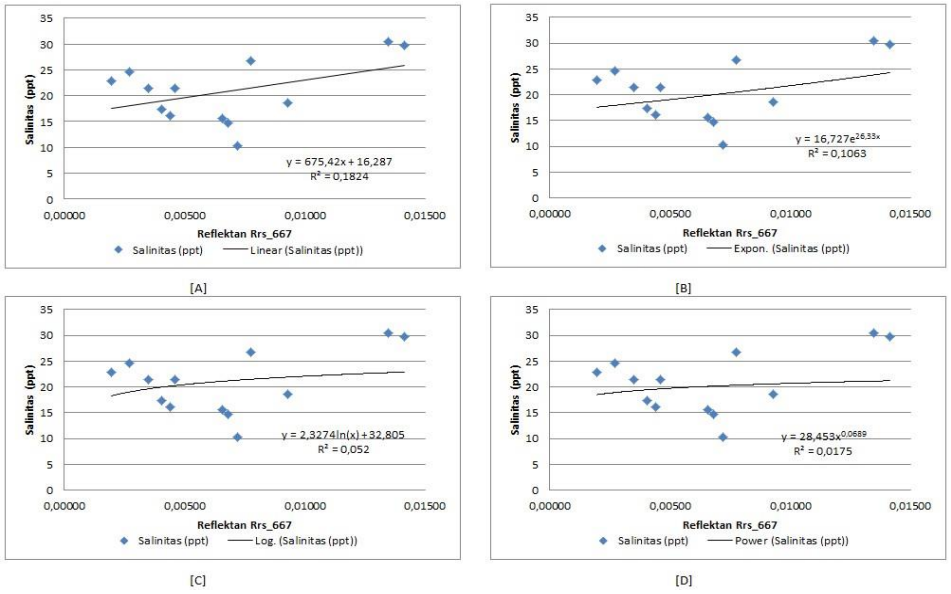

Figure 13. Results of scatter Salinity analysis of fashionable aqua images for a wavelength of 667 nm in June 2018

CONCLUSION

It can be concluded that Aqua Modis satellite image data can be used to map and analyze salinity content on the coast as part of a sustainable coastal management process. The optimal wavelength that can describe the value of coastal salinity is 443 nm wavelength nm and 531 nm wavelength both for June 2018 and for images in July 2018. Among of these mathematical models, the logarithmic model has a more optimal level than the linear, exponential and power models, where the correlation value is shown is 0.8736, which means that there are around 87.36% of the existing data can be represented in the mathematical model developed.

ACKNOWLEDGEMENT

The author would like to thank the LPPM UPN "Veteran" East Java for providing research funding so that this research can be carried out properly and correctly. Also to the civil engineering study program that has provided support for the use of the Soil Mechanics laboratory and the ease of administrative processes, and finally for younger students who have helped as surveyors in the field.

REFERENCES

Anguelova, M., & Huq, P. (2017). Effects of Salinity on Surface Lifetime of Large Individual Bubbles. *Journal of Marine Science and Engineering*, *5*(3), 41.

Arabi, B., Salama, M. S., Wernand, M. R., & Verhoef, W. (2018). Remote sensing of water constituent concentrations using time series of in-situ hyperspectral measurements in the Wadden Sea. *Remote Sensing of Environment*, *216*, 154–170.

Asfaw, E., Suryabhagavan, K. V., & Argaw, M. (2016). Soil salinity modeling and mapping using remote sensing and GIS: The case of Wonji sugar cane irrigation farm, Ethiopia. *Journal of the Saudi Society of Agricultural Sciences*.

Guo, Q., Wu, X., Bing, Q., Pan, Y., Wang, Z., Fu, Y., ... Liu, J. (2016). Study on Retrieval of Chlorophyll-a Concentration Based on Landsat OLI Imagery in the Haihe River, China. *Sustainability*, *8*(8), 758.

Jiménez-Muñoz, J. C., & Sobrino, J. A. (2008). Split-window coefficients for land surface temperature retrieval from lowresolution thermal infrared sensors. *IEEE Geoscience and Remote Sensing Letters*, *5*(4), 806–809.

Kumar, K. S., Bhaskar, P. U., & Padmakumari, K. (2012). Estimation of Land Surface Temperature To Study Urban Heat Island Effect Using Landsat Etm+ Image. *International Journal of Engineering Science and Technology*, *4*(02), 771–778.

Lee, L. E. E. H., Fredolin, T., Isabella, G. J., & Saim, S. (2017). Prediction of salinity intrusion in the sheltered estuary of TerTerengganu River in Malaysia using 1-D empirical intrusion model, *36*(5), 57–66.

Li, H., Hu, L., & Xia, Z. (2013). Impact of Groundwater Salinity on Bioremediation Enhanced by Micro-Nano Bubbles. *Materials*, *6*(9), 3676–3687.

Lymburner, L., Botha, E., Hestir, E., Anstee, J., Sagar, S., Dekker, A., & Malthus, T. (2016). Landsat 8: Providing continuity and increased precision for measuring multi-decadal time series of total suspended matter. *Remote Sensing of Environment*, *185*, 108–118.

Mathew, M. M., Srinivasa Rao, N., & Mandla, V. R. (2017). Development of regression equation to study the Total Nitrogen, Total Phosphorus and Suspended Sediment using remote sensing data in Gujarat and Maharashtra coast of India. *Journal of Coastal Conservation*, *21*(6), 917–927.

Mittaz, J., & Harris, A. (2011). A Physical Method for the Calibration of the AVHRR/3 Thermal IR Channels. Part II: An InOrbit Comparison of the AVHRR Longwave Thermal IR Channels on board *MetOp-A* with IASI. *Journal of Atmospheric and Oceanic Technology*, *28*(9), 1072–1087.

Moreno-Madrinan, M. J., Al-Hamdan, M. Z., Rickman, D. L., & Muller-Karger, F. E. (2010). Using the surface reflectance MODIS terra product to estimate turbidity in Tampa Bay, Florida. *Remote Sensing*.

Petitcolin, F. R., & Vermote, E. F. (2001). Applications of middle infrared surface reflectance from MODIS data. *IGARSS 2001. Scanning the Present and Resolving the Future. Proceedings. IEEE 2001 International Geoscience and Remote Sensing Symposium (Cat. No.01CH37217)*.

Ruello, M. R., Cinque, A., Di Donato, V., Molisso, F., Terrasi, F., & Russo Ermolli, E. (2017). The interplay between sea level rise and tectonics in the Holocene evolution of the St. Eufemia Plain (Calabria, Italy). *Journal of Coastal Conservation*, *21*(6), 903–915.

Wang, L., & Cao, C. (2008). On-Orbit Calibration Assessment of AVHRR Longwave Channels on MetOp-A Using IASI. *IEEE Transactions on Geoscience and Remote Sensing*, *46*(12), 4005–4013.

Wibisana, H., & Zainab, S. (2017). Time Series Analysis of Sea Surface Temperature With Aqua MODIS from 2011 to 2016. Case Studi: North Coast of Gresik and Madura. *IPTEK The Journal for Technology and Science*, *28*(1), 15–19.

Zhou, G., Ma, Z., Sathyendranath, S., Platt, T., Jiang, C., & Sun, K. (2018). Canopy Reflectance Modeling of Aquatic Vegetation for Algorithm Development: Global Sensitivity Analysis. *Remote Sensing*, *10*(6), 837.